SLAC-PUB-7585
August 13, 1997

A Preliminary Measurement of R_b using the Upgrade SLD Vertex Detector

The SLD Collaboration*

Stanford Linear Accelerator Center

Stanford University, Stanford, CA 94309

Abstract

We report a new measurement of R_b using data obtained during the 1996 SLD run. This measurement uses a double tag technique, where the selection of a b hemisphere is based on the reconstructed mass of the B hadron decay vertex. The method utilizes the 3D vertexing capabilities of SLD's new CCD vertex detector and the small and stable SLC beams to obtain a high b tagging efficiency and purity of $\mathbf{47.9}\%$ and $\mathbf{97.6}\%$, respectively. We obtain a preliminary result of $R_b = 0.2101 \pm 0.0034_{stat.} \pm 0.0022_{syst.} \pm 0.0003_{R_c}$ for 1996 data. With our previous measurement from 1993-95 data, we obtain a combined preliminary 93-96 result of $R_b = 0.2124 \pm 0.0024_{stat.} \pm 0.0017_{syst.}$.

Submitted to the International Europhysics Conference on High Energy Physics (HEP97), 19-26 August 1997, Jerusalem, Israel.

1 Introduction

The measurement of the fraction of hadronic Z^0 decays into bottom quarks, $R_b = \Gamma_{Z^0 \to b\bar{b}}/\Gamma_{Z^0 \to hadrons}$, provides a precision test of the standard model (SM). Since QCD and oblique (propagator) corrections are common to all quark flavors, these corrections mostly cancel in the ratio of partial widths. Therefore, given the top mass measured by D0 and CDF [1], R_b is sensitive to physics beyond the standard model which directly affects the Zbb vertex.

A previous measurement of R_b by SLD introduced the mass tag [2] to identify B hadrons with high efficiency and purity. This method of identifying B hadrons has been significantly improved utilizing SLD's upgrade vertex detector, VXD3 [3]. The VXD3 detector consists of 96 $13 cm^2$ custom made CCDs, a total of 307 Mpixels, providing a 3D space point resolution of approximately 5μm along each coordinate. The measured track impact parameter resolution is $\sigma_{r\phi}[\mu m] = 13 \oplus 38/p \sin^{3/2}\theta$, $\sigma_{rz}[\mu m] = 24 \oplus 38/p \sin^{3/2}\theta$ where p is the track momentum expressed in GeV/c. A detailed description of the SLD detector can be found elsewhere [4]. This paper presents an analysis of R_b using the mass tag for the 1996 SLD run with a total of 50k Z^0 events collected with VXD3.

2 Method

Hadronic events are divided into two hemispheres by the plane perpendicular to the thrust axis of the event. Each hemisphere is then individually tagged for the presence of a B hadron. The fraction of hemispheres tagged as originating from b quarks is given by

$$F_s = R_b\epsilon_b + R_c\epsilon_c + (1 - R_c - R_b)\epsilon_{uds}$$

and the fraction of events with both hemispheres tagged as originating from a b quark is given by

$$F_d = R_b({\epsilon_b}^2 + \lambda_b(\epsilon_b - \epsilon_b^2)) + R_c({\epsilon_c}^2 + \lambda_c(\epsilon_c - \epsilon_c^2)) + (1 - R_c - R_b){\epsilon_{uds}}^2.$$

The above two equations are solved for R_b and ϵ_b, the efficiency for tagging a B hadron. The efficiencies for tagging charm, ϵ_c, and uds, ϵ_{uds}, as well as the bottom and charm correlations for tagging both hemispheres in an event, λ_b and λ_c, respectively, are taken from Monte Carlo (MC) studies. A fixed SM value of $R_C = 0.171$ is used.

2.1 Event Selection

Hadronic event selection is based on the visible energy and track multiplicity in the event. The visible energy is measured using central drift chamber (CDC) tracks and must exceed 18 GeV. There must be at least 7 CDC tracks, 3 having associated hits in the vertex detector. We also require that the thrust axis, measured from calorimeter clusters, satisfies $|cos\theta| <$

0.71. This insures that the event is contained well within the acceptance of the vertex detector. Additionally, we restrict events to contain no more than 3 jets so that hemispheres are well defined. Jets are defined by the JADE algorithm applied to tracks with $y_{cut} = 0.02$. A total of 31204 events pass the above hadronic event selection and jet cut. Monte carlo studies indicate that there is $+0.9 \pm 0.29\%$ bias in favor of selecting $b\bar{b}$ events with these cuts. The remaining non-hadronic background is negligible at $< 0.1\%$ level.

The SLC interaction point (IP) has a size of approximately $(1.5 \times 0.8 \times 700)\mu m$ in (x,y,z). The motion of the IP xy position over a short time interval is estimated to be approximately $6\mu m$. Since this motion is smaller than the xy resolution for fitting tracks to find the primary vertex (PV) in a given event, we use the average IP position, $\langle IP \rangle$, for the x and y coordinates of the primary vertex. The average is obtained from tracks in approximately 30 sequential hadronic events. The z coordinate of the PV is determine from each event separately. This results in a PV uncertainty of $7\mu m$ transverse to the beam direction and a longitudinal uncertainty of $15\mu m$, $19\mu m$, and $32\mu m$ for uds, c, and b events, respectively. By averaging over many hadronic events to find the primary vertex xy, b-tag correlation effects between hemispheres due to PV error are significantly suppressed.

2.2 Track Selection

Reconstruction of the mass of B hadrons is preceded by first identifying secondary vertices in each hemisphere. Only tracks that are well measured are included in the vertex and mass reconstruction. Tracks are required to have at least 23 CDC hits, start within a radius of 50cm, and have a transverse momentum greater than 0.25 GeV. The CDC track is also required to extrapolate to within 1cm of the $\langle IP \rangle$ in xy and within 1.5cm of the PV in z. The fit of the CDC track must satisfy $\chi^2/d.o.f. < 8$. At least two vertex detector hits are required, the combined CDC+VXD3 fit must satisfy $\chi^2/d.o.f. < 8$, and $|cos\theta| < 0.87$. Tracks with an xy impact parameter > 3.0mm or an xy impact parameter error $> 250\mu m$ with respect to the IP are removed from consideration in the vertex and mass reconstruction.

2.3 Vertex Mass Reconstruction

Vertex identification is done using a topological vertexing method [5]. Each track is parameterized by a Gaussian resolution tube in 3D with a width equal to the uncertainty in the measured track position at the IP. Points in space where there is a significant overlap of tracks is considered as a possible vertex point. Determination of a vertex is done by clustering maxima in the overlap density distribution into vertices for separate hemispheres. Secondary vertices are found in approximately 65% of all b hemispheres, 20% for charm, and $< 1\%$ for uds hemispheres. Previously, using our vertex detector, VXD2, we find secondary vertices in approximately 50% of bottom and 16% of charm, and $< 1\%$ of light quark hemispheres.

Only vertices that are significantly displaced from the PV are considered to be possible B hadron decay vertices. We require the distance between the PV and the secondary vertex to be a factor of 5 larger than the root mean square error of the primary and secondary vertices along the PV-vertex axis.

Due to the cascade nature of the B decay, tracks from the decay may not all originate from the same space point. Therefore, a process of adding tracks to the secondary vertex has been developed to identify all B decay tracks for mass reconstruction. The criteria for adding tracks to the vertex is illustrated in figure 1a. A track is attached to the secondary vertex if

- the 3D closest approach to the PV-secondary vertex axis, T, is $< 1mm$,
- the distance along the vertex axis to this point, L, is $> 0.5mm$, and
- the $L/D > 0.25$, where D is the secondary vertex decay distance.

The first cut ensures that the added track is in close proximity to the B flight path. The second and third cuts prevent the addition of tracks that are consistent with coming from the IP.

The invariant mass of the B candidate is obtained assuming each track has the mass of a charged π. We improve the b tagging efficiency by applying a kinematic correction to the calculated invariant mass. Due to the neglect of information about the neutral particles in the decay, the SV flight path and the SV momentum vector are typically acollinear. In order to compensate for the acollinearity we correct the invariant mass using the minimum missing momentum (P_t) transverse to the SV flight path. To reject non-$b\bar{b}$ events with an artificially large P_t due to detector resolution effects, we define P_t with respect to a vector tangent to the error boundaries of both the PV and the SV, such that P_t is minimized (see Fig. 1(b)). The ability to make this minimal correction is most effective at SLD due to the small and stable beamspot of the SLC and the high resolution vertexing. We then define the P_t-corrected mass as

$$\mathcal{M} = \sqrt{M^2 + P_t^2} + |P_t|,$$

where M is the invariant mass of the vertex, and require $\mathcal{M} \leq 2 \times M$ to reduce the contamination from fake vertices in light quark events. The distribution of $\mathcal{M}$ is shown in Fig. 2. By requiring $\mathcal{M} > 2\ GeV/c^2$ we significantly increase our b-tag efficiency, yielding $\epsilon_b = 47.9\%$, while maintaining a high purity of 97.6%.

The efficiency and purity performance for tagging B hadrons as a function of mass tag is shown in figure 3. For a mass tag cut greater than 2 GeV/c^2, we obtain MC efficiencies of 48.1%, 1.21%, and 0.083% for b, c, and uds hemispheres, respectively. The b-hemisphere correlation is $\lambda_b = 0.24 \pm 0.22_{MC_{Stat.}}\%$. For the calculation of R_b at a low mass cut, where the charm fraction is significant, we find that the inclusion of charm tag hemisphere correlation has a noticeable effect. For a mass tag cut of 2 GeV/c^2, we measure R_b to be $0.2101 \pm 0.0034_{stat.}$

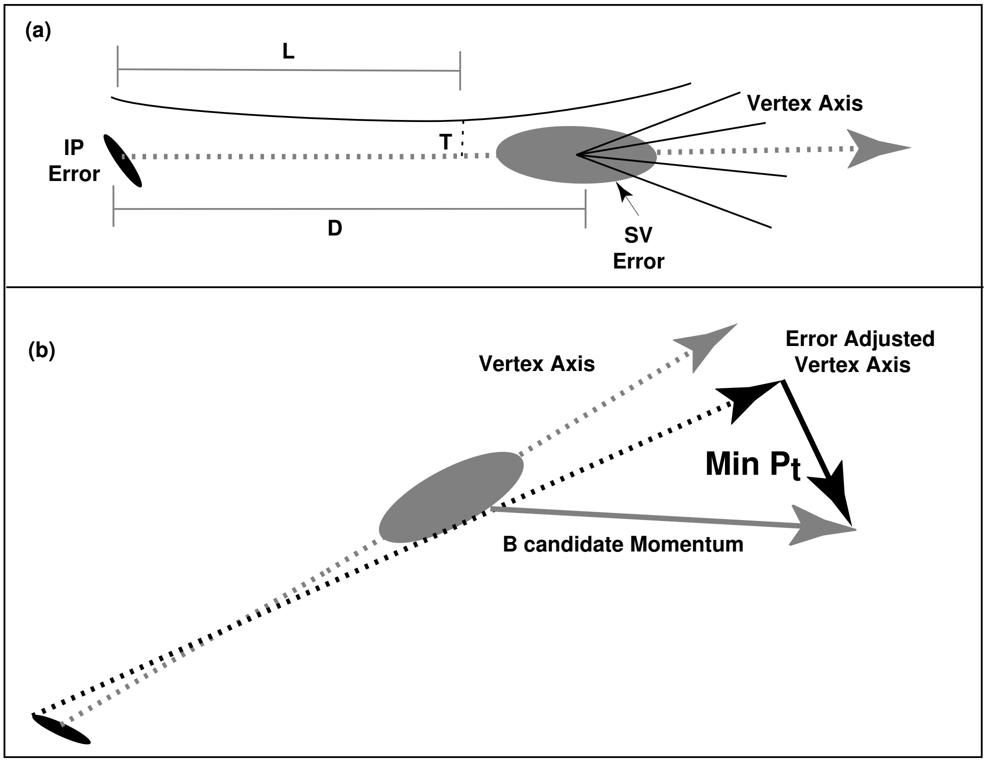

.

Figure 1: (a) An illustration of the SV track attachment criteria. (b) Illustration of the min P_t derivation.

3 Systematic Errors

The systematic uncertainty in measuring R_b is due to a combination of MC and detector related quantities. Each contribution to the error manifests itself through the charm and *uds* efficiency, charm and bottom correlations, and the assumed SM value of R_c. The systematic errors are given in Table 1 and described below.

3.1 Detector Systematic Error

The Monte Carlo contains approximately 3.5% more reconstructed tracks than the data. Therefore, tracks are randomly removed from the MC depending on the transverse momentum, P_t, ϕ, and $cos(\theta)$ of the track, so that the track multiplicity in the data and MC agree. The systematic error due to the efficiency correction is obtained by assigning an error equal

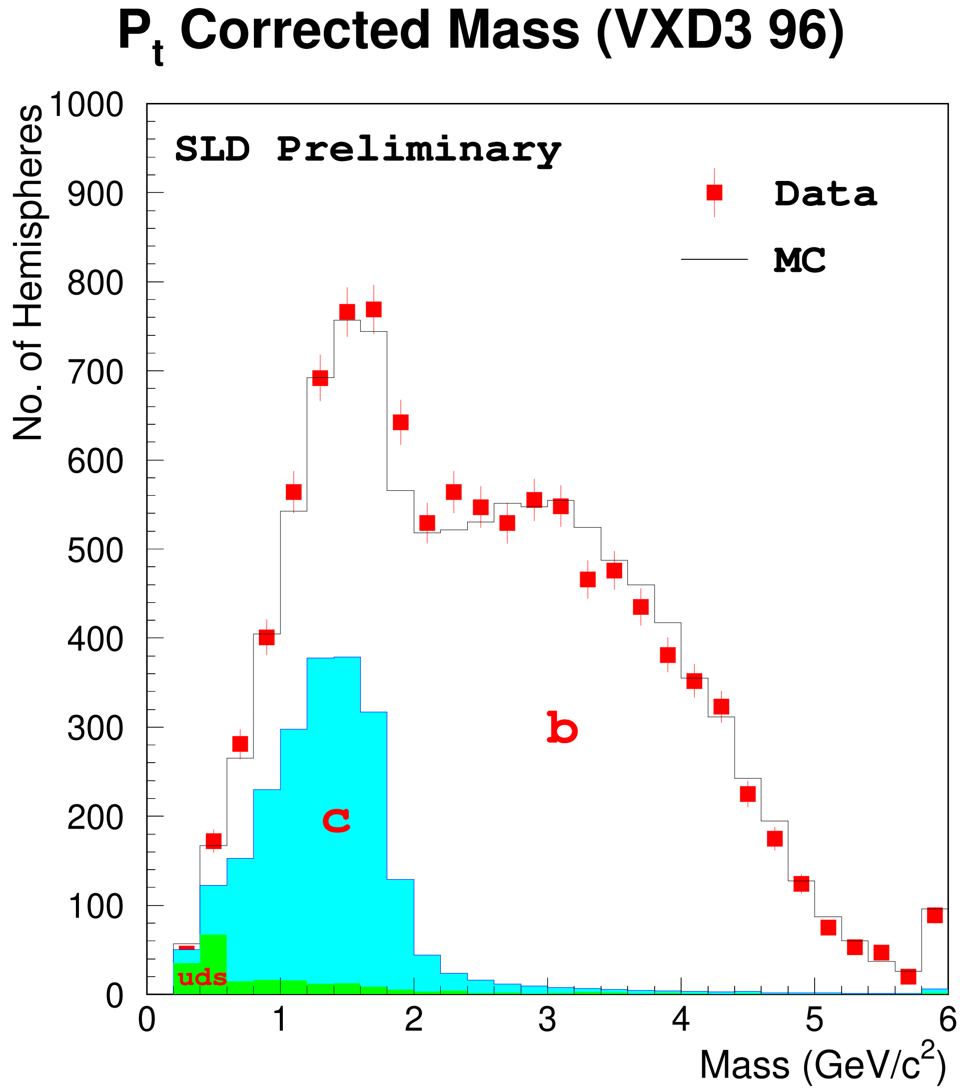

.

Figure 2: Distribution of P_t corrected mass for data (points) and MC breakdown of the b, c and uds contributions.

to the change in R_b when the analysis is done with and without these corrections.

The impact parameter resolution in the data is slightly worse than the MC due to residual alignment effects. The impact parameter distribution tails agree well between the data and MC, while the core of the MC distribution requires smearing corrections to match the data. We smear the impact parameters with a random Gaussian width of $9\mu m/sin\theta$ in xy and $10\mu m/sin^2\theta$ in rz. The full difference in R_b introduced by the smearing process is estimated as the systematic error.

3.2 Physics Systematic Error

The systematic error due to uncertainties in physics is assigned by comparing the nominal MC distributions with an alternative set of distributions based on the present world average measurement uncertainties in these physical parameters. The two significant sources of

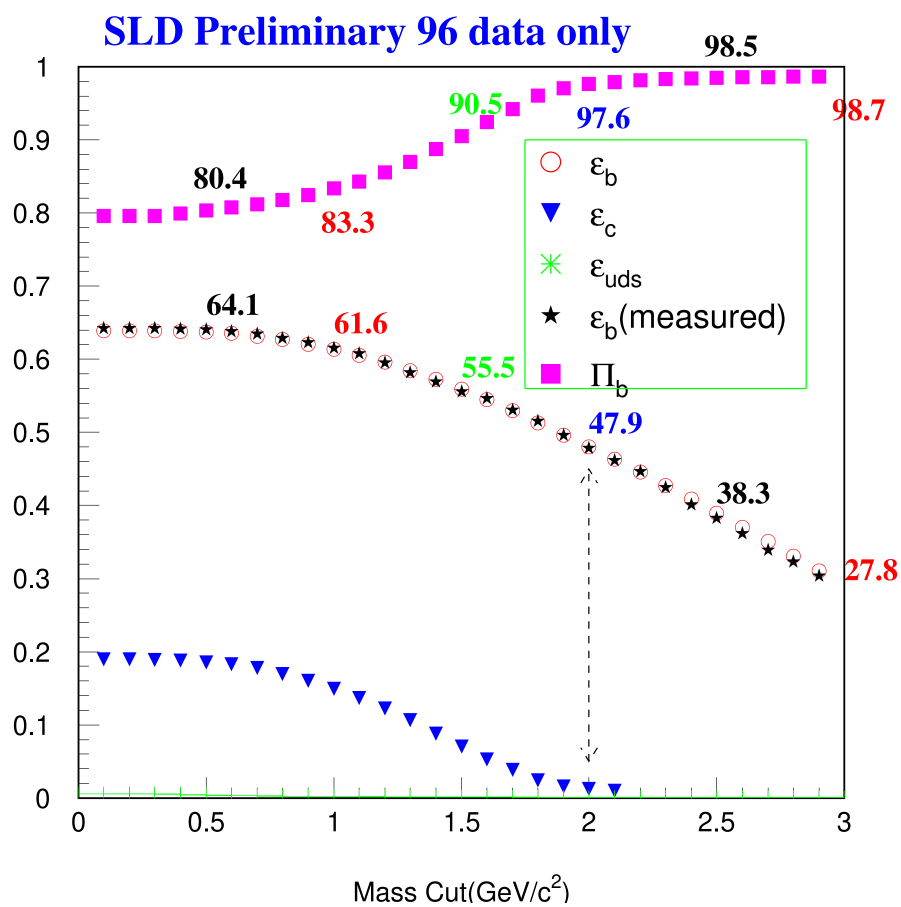

.

Figure 3: Efficiency and purity as a function of mass tag cut.

systematic errors from light quark events come from the uncertainties in long lived strange particle production and gluon splitting into heavy quark pairs. The effects of strange particle production are studied by varying the $s\bar{s}$ production probability in jet fragmentation. For gluon splitting effects, the $g \to b\bar{b}$ and $g \to c\bar{c}$ production rates are varied according to the OPAL $g \to c\bar{c}$ measurement [6] and the theoretical prediction for the ratio of $g \to b\bar{b}/g \to c\bar{c}$ [7].

The various charm hadron production rates and fragmentation parameters are varied within the present LEP measurement errors. Charm hadron fragmentation is studied by varying the average scaled energy $\langle x_E \rangle$ in the Peterson fragmentation function [8], as well as by studying the difference between Peterson model, and the Bowler model [9] with the same $\langle x_E \rangle$. Charm decay lifetimes are varied according to the world average measurement errors [10]. The charm decay charged multiplicity and K^0 production rate systematic uncertainties are based on measurements by the Mark-III measurements [11]. Charm decays with fewer neutral particles have higher charged mass and are therefore more likely to be tagged. Thus, an additional systematic uncertainty is estimated by varying the rates of charm decays

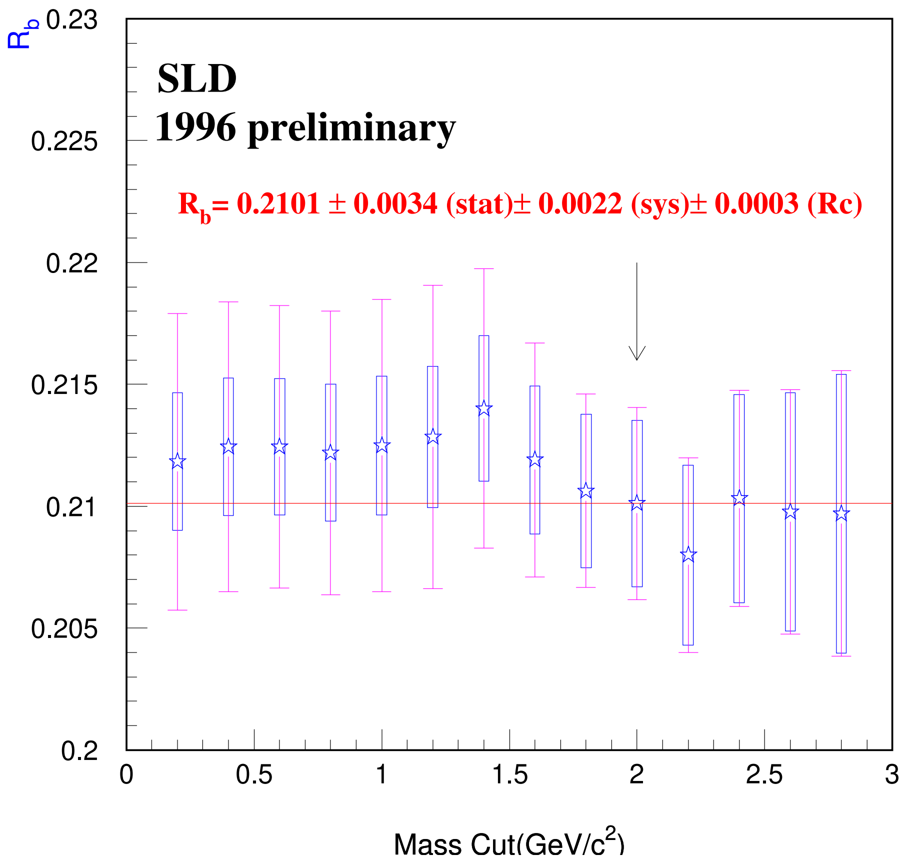

.

Figure 4: R_b as a function of mass tag cut.

with no π^0's by $\pm 10\%$.

The MC B decay modeling uncertainty enters via the λ_b estimation. It is studied by varying the B lifetime, Λ_b production rate, fragmentation function and the B decay charged multiplicity in a similar manner as for the charm systematic studies. Simulation errors which affect the tagging efficiency are studied by comparing data and MC angular distributions of the b tagging rates, and a systematic error is assigned to the difference. Hard gluon radiation effects are estimated from $\pm 30\%$ variation of the fraction of MC events where both B hadrons are contained within the same hemisphere and a hard gluon is in the other. The b tagging efficiency increases with the B hadron momentum, and there is a difference between the hemisphere momentum correlation for the HERWIG [12] and JETSET [13] event generators. Thus, an error is assigned to this difference. The various sources of error on R_b as a function of mass tag cut is shown in Figure 5.

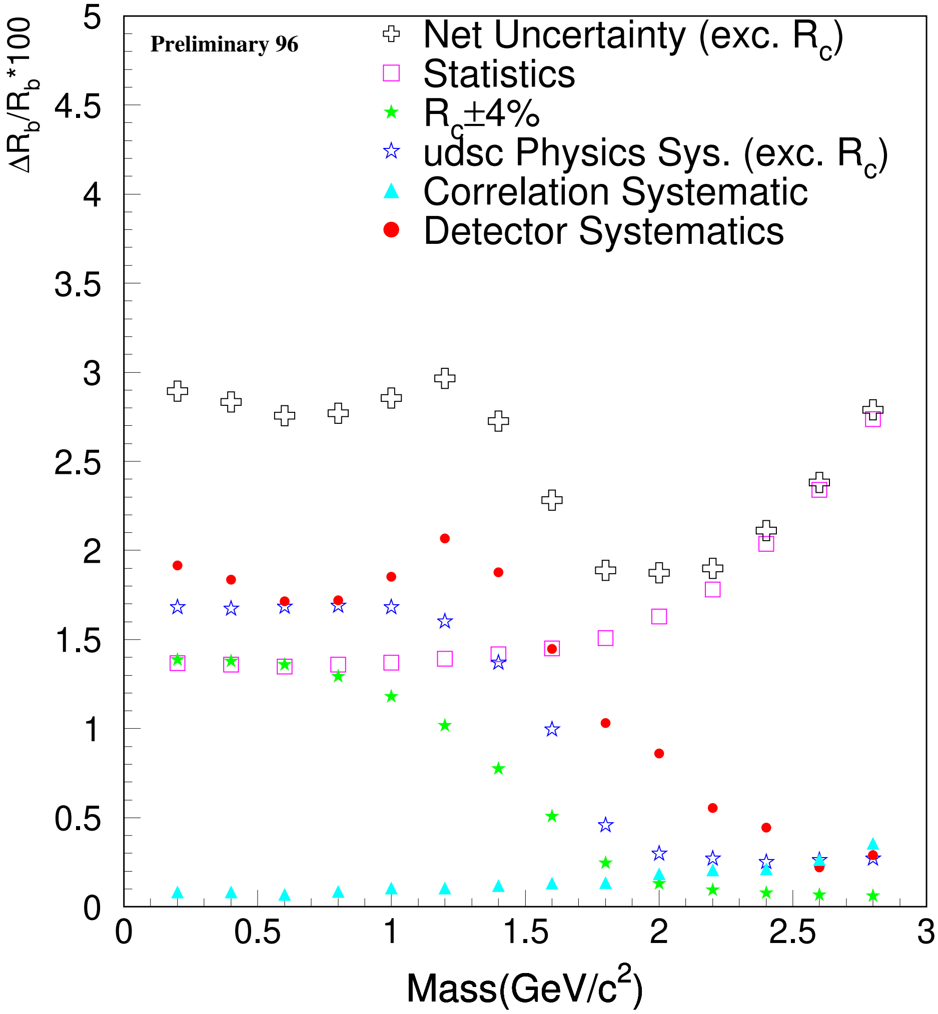

.

Figure 5: R_b statistical and systematic error as a function of mass tag cut.

4 Conclusions

We have measured R_b using a high efficiency and purity tag based on the mass of displaced vertices. With SLD's upgrade vertex detector, VXD3, we have been able to increase the efficiency for tagging B hadrons from approximately 35% for the 93-95 analysis using VXD2 to 48% with VXD3. This increase has allowed us to measure R_b with the same statistical error as our previous measurement using approximately 2.5 times less data.

Using 50k Z^0 events during the 1996 run with VXD3, we measure $R_b = 0.2101 \pm 0.0034_{stat.} \pm 0.0022_{syst.} \pm 0.0003_{R_c}$. With 150k Z^0 events obtained during 93-95 running, we measure $R_b = 0.2142 \pm 0.0034_{stat.} \pm 0.0015_{syst.} \pm 0.0002_{R_c}$. We report a combined preliminary 93-96 result of $R_b = 0.2124 \pm 0.0024_{stat.} \pm 0.0017_{syst.} \pm 0.0002_{R_c}$, where all results include a +0.0003 correction for the γ-exchange effect. This measurement is consistent with the standard model expectation of 0.2158 and with measurements at LEP [14].

References

[1] CDF Collab. F. Abe *et. al*, *Phys. Rev. Lett.* **74** (1995) 2626;
D0 Collab. S. Abachi *et. al.*, *Phys. Rev. Lett.* **74** (1995) 2637.

[2] SLD Collab. K. Abe *et al.*, *"A Measurement of the fraction R_b of $Z^0 \to b\bar{b}$ events in the hadronic Z^0 decays using a Vertex Mass Tag"*, SLAC-PUB-7481, submitted to *Physical Review Letters*

[3] K. Abe *et al.*, *"Design and Performance of the SLD Vertex Detector, a 307 Mpixel tracking System"*, SLAC-PUB-7385, submitted to *Nucl. Inst. & Meth.*

[4] SLD Collab. K. Abe *et al.*, *Phys. Rev.* **D53**, (1996) 1023.

[5] D. Jackson, *Nucl. Inst. & Meth.* **A388** (1997) 247.

[6] OPAL Collab. R. Akers *et al.*, *Phys. Lett.* **B353** (1995) 595.

[7] The LEP Electroweak Working Group, "Presentation of the LEP Electroweak Heavy Flavour Results for Summer 1996 Conferences", *LEPHF/96-01*, July 1996.

[8] C. Peterson *et al. Phys. Rev.* **D27** (1983) 105.

[9] M. G. Bowler, *Z. Phys.* **C11** (1981) 169.

[10] Particle Data Group, *Phys. Rev.* **D50**, Part I (1994).

[11] Mark-III Collab., D. Coffman *Phys Lett.* **B263** (1991) 135.

[12] G. Marchesini *et al.*, *Comput. Phys. Commun.* **67** (1992) 465.

[13] T. Sjostrand, *Comput. Phys. Commun.* **82** (1994) 74.

[14] ALEPH Collab. D. Buskulic *et al.*, *Phys. Lett.* **B313** (1993) 535; R. Barate *et al.*, *Phys. Lett.* **B401** (1997) 150; R. Barate *et al.*, *Phys. Lett.* **B401** (1997) 163
OPAL Collab. P. D. Acton *et al.*, *Z. Phys.* **C60** (1993) 579; D. Akers *et al.*, *Z. Phys.* **C65** (1994) 17; K. Ackerstaff *et al.*, *Z. Phys.* **C74** (1997) 1
DELPHI Collab. P. Abreu *et al.*, *Z. Phys.* **C66** (1995) 323, *Z. Phys.* **C70** (1996) 531.

* List of Authors

K. Abe,[19] K. Abe,[29] I. Adam,[27] T. Akagi,[27] N. Allen,[4] W.W. Ash,[27] D. Aston,[27] K.G. Baird,[16] C. Baltay,[33] H.R. Band,[32] M.B. Barakat,[33] O. Bardon,[16] T. Barklow,[27] A.O. Bazarko,[11] R. Ben-David,[33] A.C. Benvenuti,[2] G.M. Bilei,[22] D. Bisello,[21] G. Blaylock,[7] J.R. Bogart,[27] B. Bolen,[17] T. Bolton,[11] G.R. Bower,[27] J.E. Brau,[20] M. Breidenbach,[27] W.M. Bugg,[28] D. Burke,[27] T.H. Burnett,[31] P.N. Burrows,[16] W. Busza,[16] A. Calcaterra,[13] D.O. Caldwell,[6] D. Calloway,[27] B. Camanzi,[12] M. Carpinelli,[23] R. Cassell,[27] R. Castaldi,[23] A. Castro,[21] M. Cavalli-Sforza,[7] A. Chou,[27] E. Church,[31] H.O. Cohn,[28] J.A. Coller,[3] V. Cook,[31] R. Cotton,[4] R.F. Cowan,[16] D.G. Coyne,[7] G. Crawford,[27] A. D'Oliveira,[8] C.J.S. Damerell,[25] S. Dasu,[27] M. Daoudi,[27] N. De Groot,[27] R. De Sangro,[13] R. Dell'Orso,[23] M. Dima,[9] P. Dervan,[4] D.N. Dong,[16] P.Y.C. Du,[28] R. Dubois,[27] B.I. Eisenstein,[14] V. Onno Eschenburg,[18] E. Etzion,[32] S. Fahey,[10] D. Falciai,[22] C. Fan,[10] M.J. Fero,[16] K. Flood,[17] R. Frey,[20] T. Gillman,[25] G. Gladding,[14] S. Gonzalez,[16] E.L. Hart,[28] J.L. Harton,[9] A. Hasan,[4] Y. Hasegawa,[29] K. Hasuko,[29] S. Hedges,[4] S.S. Hertzbach,[17] M.D. Hildreth,[27] J. Huber,[20] M.E. Huffer,[27] E.W. Hughes,[27] X. Huynh,[27] H. Hwang,[20] Y. Iwasaki,[29] D. Jackson,[25] P. Jacques,[24] J. Jaros,[27] A.S. Johnson,[3] J.R. Johnson,[32] R.A. Johnson,[8] T. Junk,[27] R. Kajikawa,[19] M. Kalelkar,[24] Y. Kamyshkov,[28] H.J. Kang,[34] I. Karliner,[14] H. Kawahara,[27] H.W. Kendall,[16] Y. Kim,[26] M.E. King,[27] R. King,[27] R.R. Kofler,[17] N.M. Krishna,[10] R.S. Kroeger,[18] J.F. Labs,[27] M. Langston,[20] A. Lath,[16] J.A. Lauber,[10] D.W.G. Leith,[27] V. Lia,[16] X. Liu,[7] M. Loreti,[21] A. Lu,[6] H.L. Lynch,[27] J. Ma,[31] G. Mancinelli,[24] S. Manly,[33] G. Mantovani,[22] T.W. Markiewicz,[27] T. Maruyama,[27] H. Masuda,[27] E. Mazzucato,[12] A.K. McKemey,[4] B.T. Meadows,[8] G. Menegatti,[12] R. Messner,[27] P.M. Mockett,[31] K.C. Moffeit,[27] T. Moore,[33] D. Muller,[27] T. Nagamine,[27] S. Narita,[29] U. Nauenberg,[10] H. Neal,[27] M. Nussbaum,[8] Y. Ohnishi,[19] N. Oishi,[19] D. Onoprienko,[28] L.S. Osborne,[16] R.S. Panvini,[30] H. Park,[20] C.H. Park,[35] T.J. Pavel,[27] I. Peruzzi,[13] M. Piccolo,[13] L. Piemontese,[12] E. Pieroni,[23] K.T. Pitts,[20] R.J. Plano,[24] R. Prepost,[32] C.Y. Prescott,[27] G.D. Punkar,[27] J. Quigley,[16] B.N. Ratcliff,[27] T.W. Reeves,[30] J. Reidy,[18] P.L. Reinertsen,[7] P.E. Rensing,[27] L.S. Rochester,[27] P.C. Rowson,[11] J.J. Russell,[27] O.H. Saxton,[27] T. Schalk,[7] R.H. Schindler,[27] U. Schneekloth,[16] B.A. Schumm,[15] J. Schwiening,[27] S. Sen,[33] V.V. Serbo,[32] M.H. Shaevitz,[11] J.T. Shank,[3] G. Shapiro,[15] D.J. Sherden,[27] K.D. Shmakov,[28] C. Simopoulos,[27] N.B. Sinev,[20] S.R. Smith,[27] M.B. Smy,[9] J.A. Snyder,[33] H. Staengle,[9] P. Stamer,[24] H. Steiner,[15] R. Steiner,[1] M.G. Strauss,[17] D. Su,[27] F. Suekane,[29] A. Sugiyama,[19] S. Suzuki,[19] M. Swartz,[27] A. Szumilo,[31] T. Takahashi,[27] F.E. Taylor,[16] E. Torrence,[16] A.I. Trandafir,[17] J.D. Turk,[33] T. Usher,[27] C. Vannini,[xx] J. Va'vra,[27] C. Vannini,[23] E. Vella,[27] J.P. Venuti,[30] R. Verdier,[16] P.G. Verdini,[23] S.R. Wagner,[27] D.L. Wagner,[10] A.P. Waite,[27] J. Wang,[27] C. Ward,[4] S.J. Watts,[4] A.W. Weidemann,[28] E.R. Weiss,[31] J.S. Whitaker,[3] S.L. White,[28] F.J. Wickens,[25] D.C. Williams,[16] S.H. Williams,[27] S. Willocq,[27] R.J. Wilson,[9] W.J. Wisniewski,[5] M. Woods,[27] G.B. Word,[24]

T.R. Wright,[32] J. Wyss,[21] R.K. Yamamoto,[16] J.M. Yamartino,[16] X. Yang,[20]
J. Yashima,[29] S.J. Yellin,[6] C.C. Young,[27] H. Yuta,[29] G. Zapalac,[32] R.W. Zdarko,[27]
and J. Zhou[20]

[1] Adelphi University, Garden City, New York 11530
[2] INFN Sezione di Bologna, I-40126 Bologna, Italy
[3] Boston University, Boston, Massachusetts 02215
[4] Brunel University, Uxbridge, Middlesex UB8 3PH, United Kingdom
[5] California Institute of Technology, Pasadena, California 91125
[6] University of California at Santa Barbara, Santa Barbara, California 93106
[7] University of California at Santa Cruz, Santa Cruz, California 95064
[8] University of Cincinnati, Cincinnati, Ohio 45221
[9] Colorado State University, Fort Collins, Colorado 80523
[10] University of Colorado, Boulder, Colorado 80309
[11] Columbia University, New York, New York 10027
[12] INFN Sezione di Ferrara and Università di Ferrara, I-44100 Ferrara, Italy
[13] INFN Lab. Nazionali di Frascati, I-00044 Frascati, Italy
[14] University of Illinois, Urbana, Illinois 61801
[15] Lawrence Berkeley Laboratory, University of California, Berkeley, California 94720
[16] Massachusetts Institute of Technology, Cambridge, Massachusetts 02139
[17] University of Massachusetts, Amherst, Massachusetts 01003
[18] University of Mississippi, University, Mississippi 38677
[19] Nagoya University, Chikusa-ku, Nagoya 464 Japan
[20] University of Oregon, Eugene, Oregon 97403
[21] INFN Sezione di Padova and Università di Padova, I-35100 Padova, Italy
[22] INFN Sezione di Perugia and Università di Perugia, I-06100 Perugia, Italy
[23] INFN Sezione di Pisa and Università di Pisa, I-56100 Pisa, Italy
[24] Rutgers University, Piscataway, New Jersey 08855
[25] Rutherford Appleton Laboratory, Chilton, Didcot, Oxon OX11 0QX United Kingdom
[26] Sogang University, Seoul, Korea
[27] Stanford Linear Accelerator Center, Stanford University, Stanford, California 94309
[28] University of Tennessee, Knoxville, Tennessee 37996
[29] Tohoku University, Sendai 980 Japan
[30] Vanderbilt University, Nashville, Tennessee 37235
[31] University of Washington, Seattle, Washington 98195
[32] University of Wisconsin, Madison, Wisconsin 53706
[33] Yale University, New Haven, Connecticut 06511
[33] Yale University, New Haven, Connecticut 06511
[34] Sogang University, Seoul, Korea
[35] Soongsil University, Seoul, Korea

Light Quark Systematic (ϵ_{uds})	δR_b
$g \to b\bar{b}$ 0.31±0.11%	-0.00040
$g \to c\bar{c}$ 2.38±0.48%	-0.00038
K^0 production ±10%	-0.00002
Total *uds* physics systematic	**0.00056**
Charm Systematic (ϵ_c)	δR_b
D^+ production 0.259 ± 0.028	-0.00004
D_s production 0.115 ± 0.037	-0.00006
c-baryon production 0.074 ± 0.029	0.00017
c-frag. $\langle x_E \rangle_D = 0.482 \pm 0.008$	-0.00002
D^0 lifetime 0.415 ± 0.004 ps	-0.00003
D^+ lifetime 1.057 ± 0.015 ps	-0.00001
D_s lifetime 0.467 ± 0.017 ps	-0.00003
Λ_c lifetime 0.200 ± 0.011 ps	-0.00001
D decay multiplicity	-0.00018
$D \to K^0$ production	+0.00025
D decay no-π^0 frac.	+0.00004
Total Charm Physics systematic	**0.00036**
B decay modeling (λ_b)	δR_b
B lifetime ±0.05 ps	0.00002
B decay $\langle N_{ch} \rangle = 5.73 \pm 0.35$	0.00015
b fragmentation	0.00034
Λ_b production fraciton 0.074 ± 0.03	0.00008
Hard gluon radiation	0.00001
B momentum correlation	0.00007
b-tag $\cos\theta$ dependency	0.00001
Total $b\bar{b}$ Physics systematic	**0.00039**
Detector Systematic	δR_b
Tracking resolution	0.00179
Tracking efficiency	0.00039
$\langle IP \rangle_{xy}$ smear	0.00013
MC statistics	0.00064
Event selection bias	0.00060
Total detector and MC	**0.00204**
$R_c = 0.171 \pm 0.006$	**0.00028**
Total (excl. R_c**)**	**0.00218**

Table 1: Summary of systematic uncertainties for the $\mathcal{M} > 2.0$ GeV/c^2 cut.